

## Spatial distributions of near-band-gap uv and yellow emission on MOCVD grown GaN epilayers

L. W. Tu and Y. C. Lee

*Department of Physics, National Sun Yat-Sen University, Kaohsiung, Taiwan 80424, Republic of China*

D. Stocker and E. F. Schubert

*Department of Electrical and Computer Engineering, Photonics Research Center, Boston University, Boston, Massachusetts 02215*

(Received 29 December 1997)

Near-band-gap UV and yellow band emission from metal-organic chemical vapor deposition grown GaN films on sapphires are investigated under laser excitation. The intensities of the UV and the yellow peaks increase at different rates as the entrance slit width of the spectrometer increases. The spatial distribution of the luminescence emission is analyzed through the dependence of photoluminescence intensity on the slit widths of the spectrometer. The yellow emission originates from a spot with a size about 1.5 times larger in diameter than the UV emission. Using an absorption mechanism, a Lorentzian line-shape distribution fit with the data gives estimated effective absorption coefficients of  $47\text{ cm}^{-1}$  for the UV signal at 364 nm and of  $32\text{ cm}^{-1}$  for the yellow signal at 546 nm, which agrees perfectly with the ones from an exponential decay fit. Dependence of UV-to-yellow peak ratio on the slit widths of the spectrometer, and consistency with possible origins of yellow luminescence is discussed. [S0163-1829(98)03132-4]

### I. INTRODUCTION

Since the first commercial green  $\text{In}_x\text{Ga}_{1-x}\text{N}$  light-emitting diode was realized,<sup>1</sup> research on wide-band-gap semiconductors based on nitrogen-related III-V compounds has accelerated tremendously.<sup>2-12</sup> Continuous wave operation of  $\text{In}_x\text{Ga}_{1-x}\text{N}$  multiple-quantum-well laser diode at room temperature has been announced with commercial-to-be performance achieved recently.<sup>13</sup> With the promising possibilities of products made from N-based materials, like full color flat panel displays, ultrahigh density storage devices, and high-temperature, high radiative-endurance devices, research topics are never lacking. Some current research areas include lowering the threshold voltage, minimizing the threshold current, increasing doping levels,<sup>14</sup> finding good Ohmic contacts,<sup>15,16</sup> reducing the defect density, and searching for proper ways of etching. Among them, one fundamental and important issue is the ability to grow good GaN films. In the studies of photoluminescence (PL) on GaN films, there is a broad emission band near 2.3 eV (yellow emission), in addition to the large, sharp, near-band-gap PL emission peak at 3.4 eV (UV emission).<sup>17,18</sup> While the search for the true origin of the yellow band emission is still a very active research area, most agree that its existence is due to defect/impurity assisted transitions and is an indicator of the quality of the films.<sup>19</sup> Reports on the studies of the near-band-gap UV and the yellow emission are plenty, including, for example, UV-to-yellow emission ratio (UV/yellow) analysis with bimolecular model.<sup>20</sup> In this work, we investigate the PL intensity of the UV and the yellow emission in detail by the simple concept of varying the slit width of the spectrometer. We analyze the involvement in comparing the UV to yellow emission peaks. Detailed analysis of the results allows us to obtain decay lengths of the UV and the yellow emission on the sample. Our results are consistent with deep-level models of yellow luminescence.<sup>19</sup>

### II. EXPERIMENTS

The samples are metal-organic chemical vapor deposition grown GaN epilayers on the *c* plane of a 2-in. sapphire substrate. The GaN film is *n* type with a doping concentration of  $1 \times 10^{18}\text{ cm}^{-3}$ . The film thickness is nominally  $2\text{ }\mu\text{m}$ . PL measurements use a 325 nm HeCd laser beam as the excitation source. Luminescence emission from the sample is collected with two plano-convex lenses *L1* and *L2* with focal lengths of 2 and 4 in., respectively. Lens separation is from 14 to 42 cm. The luminescence emission spot is located at the focal point of lens *L1*, which sends a nearly parallel beam to lens *L2*. Lens *L2* focuses the luminescence beam into the entrance slit of the spectrometer. The spectrometer is a SPEX model with a photomultiplier tube (PMT) detector (Hamamatsu R-928). Because of the chromatic dispersion of lenses *L1* and *L2*, their positions are slightly adjusted for the optimized collection of UV and yellow light. Entrance slit width of the spectrometer is varied from 10 to 3000  $\mu\text{m}$  during the PL measurements. The exit slit (the slit in front of the PMT detector) width is kept wide open at 3000  $\mu\text{m}$ . Both the entrance and the exit slit height are set at 2 cm. All measurements are done at room temperature.

### III. RESULTS AND DISCUSSION

A typical PL spectrum is shown in Fig. 1. A high-intensity, sharp peak situated at 364 nm is due to the near-band-gap transition that is in the wavelength of UV, so as to be called the UV peak. While the other broad, less intense peak around 546 nm (see the inset in the logarithmic scale) is due to the defect/impurity related transitions. This peak is centered around the yellow portion of the visible spectrum, so as to be called the yellow peak. While the true origin of the yellow emission is not clear yet, the PL intensity ratio between the UV and the yellow emission is commonly used as an indicator of the quality of a GaN sample. Knowing that

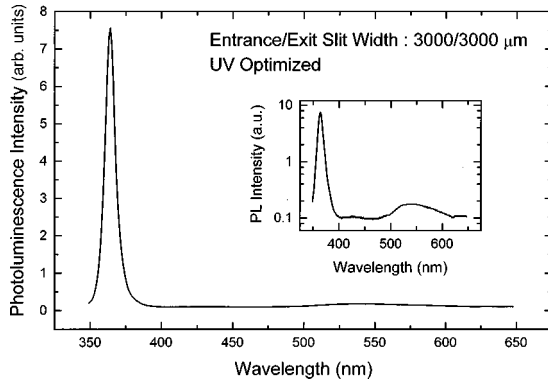


FIG. 1. Photoluminescence spectrum of GaN film grown on the  $c$  plane of sapphire substrate. Excitation source is a 325 nm He-Cd laser. The scan is UV optimized. The inset is on a logarithm scale to show the yellow emission band.

the UV light has a larger refractive index than the yellow light, the optimized lens setup will be different between the UV and the yellow peak measurements. As shown in Fig. 2, an optimized lens position for the UV peak will not be the best geometry for the yellow emission. Thus, to optimize the yellow peak signal collected by the spectrometer, the lens  $L1$  has to be moved away from the sample relative to the best position for the UV signal due to chromatic dispersion. The PL spectrum shown in Fig. 1 is a single scan over the whole wavelength range under UV optimized condition.

The inset in Fig. 3 shows the UV PL peak intensity versus the entrance slit width of the spectrometer. The UV peak intensity increases with the slit width and flattens out beyond about 1000  $\mu\text{m}$ . Treating the spatial emission distribution as in two dimensions, it gives

$$I(x,y) = I_0 \exp[-\alpha(x^2 + y^2)^{1/2}], \quad (1)$$

where  $\alpha$  is the effective absorption coefficient,  $x$  corresponds to the slit width, and  $y$  corresponds to the slit height. Then, the measured peak intensity shown in the inset is actually an integration of the luminescence emission intensity over the range of the slit opening, i.e., a two-dimensional integration of  $I(x,y)$  with respect to  $y$  from  $-1$  to  $1$  cm, and then, with respect to  $x$  from  $-(\text{slit width})/2$  to  $(\text{slit width})/2$ . Since an

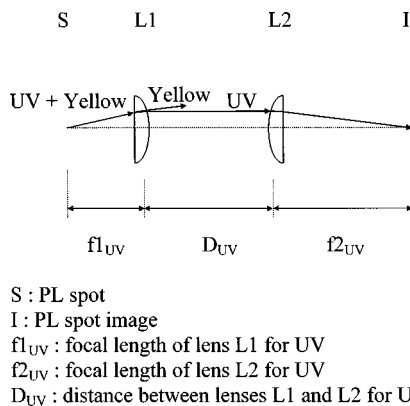


FIG. 2. Ray tracing to show the UV and the yellow luminescence emission. Chromatic dispersion is schematically shown. While the figure shows an optimized geometry for the UV signal, the geometry is not proper for the yellow emission collection.

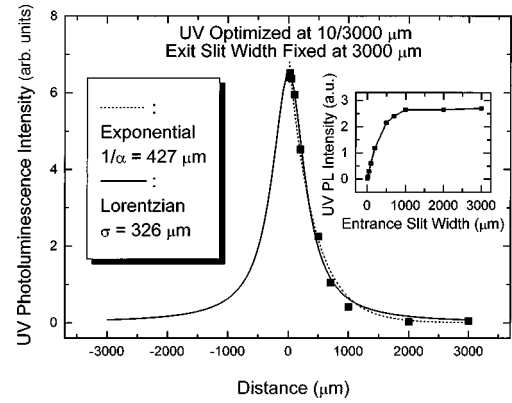


FIG. 3. UV PL signal intensity versus the entrance slit width is shown in the inset. The main figure is the derivative of the curve shown in the inset with respect to the slit width and approximates the UV emission intensity distribution centered at the laser spot.

analytical form is not obtainable with respect to the integration of  $y$ , we can obtain an empirical result from the derivative of the UV intensity of the inset with respect to the slit width as shown in Fig. 3, which approximates the UV emission intensity distribution on the sample along the  $x$  direction. Since the collecting lenses  $L1$  and  $L2$  have different focal lengths  $f1 = 2$  in. and  $f2 = 4$  in., respectively, there is a magnification factor  $M = f2/f1 = 2$  that has to be included in the calculations of the luminescence emission spot size on the sample, which, in turn, yields the effective absorption coefficients. An excellent fit with a Lorentzian distribution function

$$L(x) = \frac{\sigma}{\pi(\sigma^2 + x^2)}, \quad (2)$$

where  $2\sigma$  is the full width at half maximum, gives a  $\sigma$  of 326  $\mu\text{m}$ . On the other hand, applying the exponential decay equation in one dimension

$$I(x) = I(0) \exp(-\alpha x), \quad (3)$$

to fit Fig. 3 gives an estimated decay length,  $1/\alpha$ , of 427  $\mu\text{m}$ , which gives an effective absorption coefficient of  $46.8 \text{ cm}^{-1}$  after dividing 427  $\mu\text{m}$  by 2, the magnification factor. In the Lorentzian fit, the value of  $L$  drops to  $1/e$  of the maximum value at  $x = \sqrt{e-1}\sigma$ . The inverse of  $\sqrt{e-1}\sigma/2$  yields  $46.8 \text{ cm}^{-1}$ , which is exactly the same as the previous value deduced from the exponential equation. Taking  $\sqrt{e-1}\sigma$  as the estimated effective spot size of the UV emission on the GaN film, it gives a value of 427  $\mu\text{m}$ .

The slit width dependence of the yellow emission is shown in the inset of Fig. 4. The PL intensity of the yellow peak increases with the slit width and does not saturate until about 2000  $\mu\text{m}$ . Employing the same empirical approach and taking a derivative of the yellow peak PL intensity with respect to the entrance slit width generates Fig. 4, which reflects the yellow emission distribution profile on the sample. The actual intensity distribution spread on the sample is half of what is shown in Fig. 4 taking into account the magnification factor of 2. An exponential fit gives an estimated effective decay length,  $1/\alpha$ , of 633  $\mu\text{m}$ , which then gives an effective absorption coefficient of  $31.6 \text{ cm}^{-1}$  while the

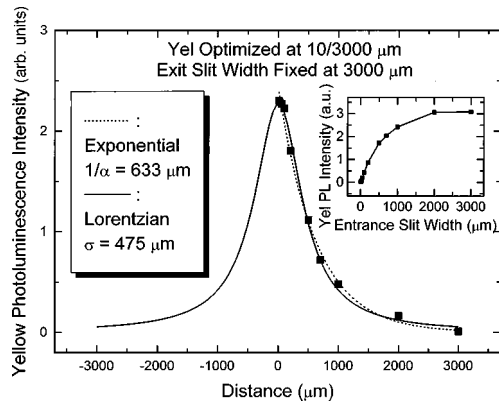


FIG. 4. Yellow PL signal intensity versus the entrance slit width is shown in the inset. The main figure is the derivative of the curve shown in the inset and approximates the yellow emission intensity distribution centered at the laser spot, which spreads over a wider region than the UV shown in Fig. 3.

Lorentzian fit gives  $32.2 \text{ cm}^{-1}$  with the effective yellow emission spot size of  $\sqrt{e-1}\sigma = 622 \text{ }\mu\text{m}$ . Comparing Fig. 4 with Fig. 3, it can be seen that the yellow emission region is larger in diameter than the UV emission region by a factor of  $\sim 1.5$ . Due to the finite distance between lens  $L1$  and  $L2$ , light emitted off the focal point of lens  $L1$  may not be fully collected by the lens  $L2$ . Taking this geometric factor into the calculation will increase the effective decay lengths of the UV and the yellow emission, and will increase the spot size ratio between the yellow and the UV emission, too. On the other hand, by using the one-dimensional exponential decay function to approximate the two-dimensional one gives larger decay lengths. During the fitting process, Gaussian distribution function was tested to fit the luminescence emission distribution profile on the sample, but the fitting results are much worse than those from the exponential and the Lorentzian function, which is the best fit among the three.

Possible mechanisms that explain the size difference between the UV and the yellow emission are discussed here along two major reasoning. First is absorption mechanism related, that is, UV (or yellow) light is generated within the laser-hitting spot, travels along and is absorbed through loss processes within an effective absorption length. In this mechanism, the size difference is due to different absorption coefficients, and this is what is used to analyze our data. Besides, UV light might be reabsorbed through deep-level transitions and then give out yellow emission. This reabsorption-reemission, photon-recycling process could cause the size difference. From this point of view, our results are consistent with deep-level recombination models of yellow luminescence. Second is diffusion mechanism related, that is, electron-hole pairs are generated within the laser-hitting spot, diffuse through the GaN film, and then recombine to produce UV emission. In this mechanism, the size difference is due to different diffusion lengths although it is unclear in the yellow emission about the corresponding part of the electron-hole pairs associated with the UV emission. Reabsorption-reemission process after recombinations of diffused electron-hole pairs may still be the reason that causes the larger yellow emission spot. Laser beam scattering is

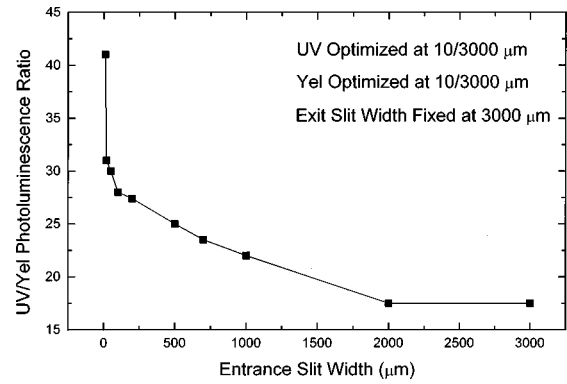


FIG. 5. Photoluminescence intensity ratio between the UV and the yellow peak. The ratio is slit width dependent.

another possible effect that could cause a larger UV (or yellow) emission area than the laser spot.

Since the refractive index of GaN at 364 nm is greater than at 546 nm by  $\sim 1\%$ , the yellow emission angle from the GaN film surface is smaller than the UV emission angle, so that, this effect can only reassure the results of larger yellow spot size. Another consideration is the focusing capability of the lenses. Estimated focused laser beam spot diameter is  $\sim 100 \text{ }\mu\text{m}$ . And, with the  $L1$ - $L2$  lens geometry used, we conclude that the focusing capability should not change our discussion.

Figure 5 shows the PL signal intensity ratio between the UV and the yellow peaks. Due to the different sizes of the PL emission region for the UV and the yellow signal, the UV/yellow signal ratio changes according to the slit width of the spectrometer. When the slit width is wide open at 3000  $\mu\text{m}$ , both the UV and yellow emission enter the slit. As the slit width narrows down, the yellow emission, which emits from a larger region than the UV, starts to be blocked by the blades of the slit, and only part of the yellow signal enters the spectrometer while the UV signal is less affected. In order to make sure that both the UV and the yellow emission are collected, both signals are optimized at an entrance slit width of 10  $\mu\text{m}$ . This optimization procedure is critical in determining the ratio of UV/yellow properly. If only the UV signal is optimized, the UV/yellow ratio can be more than one order of magnitude higher than the value shown in Fig. 5, although the fact that the UV/yellow ratio increases as the slit width narrows still remains.

#### IV. CONCLUSIONS

In conclusion, a simple and elegant technique is demonstrated to investigate the spatial profile of the UV and the yellow PL emission from GaN epilayers by varying the slit width of the spectrometer using a typical PL measurement setup. Empirically, both the Lorentzian and the exponential distribution give an excellent fit to the luminescence emission intensity profile, which yields effective absorption coefficients of  $47 \text{ cm}^{-1}$  for the UV peak at 364 nm and of  $32 \text{ cm}^{-1}$  for the yellow peak at 546 nm. The PL intensity ratio between the UV and the yellow emission depends on the slit width of the spectrometer. The increase of the UV/yellow ratio with decreasing slit width is explained by the different sizes of the emission region of the UV and the

yellow luminescence. The effective yellow emission spot size is 622  $\mu\text{m}$ , which is about 1.5 times larger in diameter than the UV spot size. This is consistent with deep-level models of yellow luminescence through the reabsorption-reemission approach. Chromatic dispersion is an important factor in optimizing the signals to ensure the proper collection of the emission at different wavelengths. Substantial improvement on the value of decay lengths could be done by using the two-dimensional exponential decay function in-

stead of the one-dimensional one through numerical method. Absorption analysis is performed on our data, and other mechanisms need further investigations.

#### ACKNOWLEDGMENTS

One of the authors (L.W.T.) would like to acknowledge support from the National Science Council of the Republic of China under Project No. NSC 87-2112-M-110-003.

- 
- <sup>1</sup>S. Nakamura, M. Senoh, N. Iwasa, S. Nagahama, T. Yamada, and T. Mukai, *Jpn. J. Appl. Phys., Part 1* **34**, L1332 (1995).
- <sup>2</sup>H. Siegle, P. Thurian, L. Eckey, A. Hoffmann, C. Thomsen, B. K. Meyer, H. Amano, I. Akasaki, T. Detchprohm, and K. Hiramatsu, *Appl. Phys. Lett.* **68**, 1265 (1996).
- <sup>3</sup>F. Hamdani, A. Botchkarev, W. Kim, H. Morkoç, M. Yeadon, J. M. Gibson, S.-C. Y. Tsen, D. J. Smith, D. C. Reynolds, D. C. Look, K. Evans, C. W. Litton, W. C. Mitchel, and P. Hemenger, *Appl. Phys. Lett.* **70**, 467 (1997).
- <sup>4</sup>C. J. Sun, J. W. Yang, B. W. Lim, Q. Chen, M. Z. Anwar, M. A. Khan, A. Osinsky, H. Temkin, and J. F. Schetzina, *Appl. Phys. Lett.* **70**, 1444 (1997).
- <sup>5</sup>R. Klann, O. Brandt, H. Yang, H. T. Grahn, and K. H. Ploog, *Appl. Phys. Lett.* **70**, 1808 (1997).
- <sup>6</sup>Y. Xin, P. D. Brown, C. J. Humphreys, T. S. Cheng, and C. T. Foxon, *Appl. Phys. Lett.* **70**, 1308 (1997).
- <sup>7</sup>N. V. Edwards, S. D. Yoo, M. D. Bremser, T. W. Weeks, Jr., O. H. Nam, R. F. Davis, H. Liu, R. A. Stall, M. N. Horton, N. R. Perkins, T. F. Kuech, and D. E. Aspnes, *Appl. Phys. Lett.* **70**, 2001 (1997).
- <sup>8</sup>C.-K. Sun, F. Vallée, S. Keller, J. E. Bowers, and S. P. DenBaars, *Appl. Phys. Lett.* **70**, 2004 (1997).
- <sup>9</sup>W. Shan, B. D. Little, J. J. Song, Z. C. Feng, M. Schuman, and R. A. Stall, *Appl. Phys. Lett.* **69**, 3315 (1996).
- <sup>10</sup>W. Shan, R. J. Hauenstein, A. J. Fischer, J. J. Song, W. G. Perry, M. D. Bremser, R. F. Davis, and B. Goldenberg, *Phys. Rev. B* **54**, 13 460 (1996).
- <sup>11</sup>C. B. Vartuli, S. J. Pearton, J. W. Lee, C. R. Abernathy, J. D. Mackenzie, J. C. Zolper, R. J. Shul, and F. Ren, *J. Electrochem. Soc.* **143**, 3681 (1996).
- <sup>12</sup>S. N. Mohammad, Z. F. Fan, A. Salvador, Ö. Aktas, A. E. Botchkarev, W. Kim, and H. Morkoç, *Appl. Phys. Lett.* **69**, 1420 (1996).
- <sup>13</sup>S. Nakamura, M. Senoh, S. Nagahama, N. Iwasa, T. Yamada, T. Matsushita, Y. Sugimoto, and H. Kiyoku, *Appl. Phys. Lett.* **70**, 1417 (1997).
- <sup>14</sup>W. Götz, N. M. Johnson, J. Walker, D. P. Bour, and R. A. Street, *Appl. Phys. Lett.* **68**, 667 (1996).
- <sup>15</sup>J. S. Foresi and T. D. Moustakas, *Appl. Phys. Lett.* **62**, 2859 (1993).
- <sup>16</sup>A. T. Ping and M. A. Khan, and I. Adesida, *J. Electron. Mater.* **25**, 819 (1996).
- <sup>17</sup>J. T. Liu, N. R. Perkins, M. N. Horton, J. M. Redwing, M. A. Tischler, and T. F. Kuech, *Appl. Phys. Lett.* **69**, 3519 (1996).
- <sup>18</sup>T. Suski, P. Perlin, H. Teisseyre, M. Leszczynski, I. Grzegory, J. Jun, M. Bockowski, S. Porowski, and T. D. Moustakas, *Appl. Phys. Lett.* **67**, 2188 (1995).
- <sup>19</sup>E. F. Schubert, I. D. Goepfert, and J. M. Redwing, *Appl. Phys. Lett.* **71**, 3224 (1997).
- <sup>20</sup>W. Grieshaber, E. F. Schubert, I. D. Goepfert, R. F. Karlicek, Jr., M. J. Schurman, and C. Tran, *J. Appl. Phys.* **80**, 4615 (1996).